Catalysis Communications 43 (2014) 218–222

Contents lists available at ScienceDirect

Catalysis Communications

journal homepage: www.elsevier.com/locate/catcom

Short Communication

Synthesis of the nanosized MCM-22 zeolite and its catalytic performance in methane dehydro-aromatization reaction

Xiaoyan Yin [a,*], Naibo Chu [b], Jianhua Yang [c], Jinqu Wang [c], Zhongfang Li [a]

[a] School of Chemical Engineering, Shandong University of Technology, Zibo 255049, PR China
[b] The Central Research Institute of Yantai WH Polyurethane Co. Ltd., Yantai 264002, PR China
[c] School of Chemical Engineering, Dalian University of Technology, Dalian 116012, PR China

ARTICLE INFO

Article history:
Received 16 April 2013
Received in revised form 18 July 2013
Accepted 8 October 2013
Available online 16 October 2013

Keywords:
MCM-22 zeolite
Nanocrystals
Methane dehydro-aromatization
Mo/HMCM-22-NZ
Durability of catalyst

ABSTRACT

A novel and facile synthesis method based on the combination of self-assembly and in-situ crystallization is developed for the preparation of nanosized MCM-22 zeolites (simplified as MCM-22-NZ hereafter) of about 40 nm, where the cationic polymer, PDDA, was added to play a role of protecting agent to avoid the synthesis colloids self-aggregation. MCM-22-NZ was characterized by XRD, TEM, DLS, NH_3-TPD, XRF, TG and N_2 adsorption analysis. The catalytic activity of MCM-22-NZ in methane dehydro-aromatization (MDA) reaction was also studied. Mo/HMCM-22-NZ showed better methane conversion, higher benzene yield and more considerable durability of the catalyst as compared to the conventional microsized catalyst.

1. Introduction

Recently, methane dehydro-aromatization (MDA) reaction has attracted increasing attention since it can directly convert methane into high value-added chemicals like benzene, toluene and naphthalene. It has been considered as one of the greatest potential technologies for effective utilization of natural gas [1–6]. Up to now, Mo/HMCM-22 catalyst is one of the most promising catalysts in MDA reaction due to its unusual channel structure and features with a higher yield of benzene and a less yield of naphthalene in comparison with the Mo/HZSM-5 catalyst under the same experimental conditions [1,6].

MCM-22 zeolite possesses two independent multidimensional channel systems: two-dimensional 10-ring sinusoidal inter-layer channel system and inter-layer channel system containing 12-ring interlayer super-cages with inner free space of 0.71 × 0.71 × 1.82 nm, both of which are accessible through 10-ring apertures [7]. Due to its unique structure and physicochemical properties, MCM-22 has been widely used in many hydrocarbon catalytic transforming processes such as isomerization, alkylation, aromatization and cracking [1,6,8–10]. However, in MDA reaction, the methane conversion decreased drastically with time-on-stream due to the heavy carbonaceous deposits on the MCM-22 catalyst, which is a vital drawback for the reaction. Therefore, many researchers have focused on how to improve the catalyst stability or to develop unusual catalysts with high catalytic performance [11–13].

It is well known that the nanosized zeolites have substantial changes in the catalytic properties, such as larger external surface areas, higher surface activity, shorter diffusion path lengths, and lower tendencies to carbon deposition in comparison to the ordinary micro-sized zeolite crystals [14–17]. Two main different methods of zeolite nanocrystals synthesis have been well summarized in the excellent review articles [14,15]. One is to synthesize the nanosized zeolites from clear solutions and gels by careful controlling of the exact synthesis parameters such as the synthesis solution composition or crystallization temperature and time [18,19]. The other method is to crystallize nanosized zeolites within an inert matrix (carbon black particles or colloid-imprinted carbons) which provides a steric hindered space for zeolite crystal growth [20,21]. With the later method, nano-zeolite with size-tailoring and uniform crystal size distributions can be prepared easily. However, there is still a high requirement for the precursor solution with clear and a low viscosity to make sure the entrance for zeolite gel into the mesopores of the matrix [20], which limits the application of the confined space synthesis method. For example, it is not suitable for the colloidal MCM-22 zeolite synthesis system. So far, the preparation and catalytic property of MCM-22 nanosized zeolites (MCM-22-NZ) have not been reported.

Taking into account the colloidal synthesis system of MCM-22, a novel and facile strategy for the nanocrystalline MCM-22 zeolite synthesis which combines self-assembly with in-situ crystallization techniques is proposed in this paper. In this route, polydiallydimethylammonium chloride (PDDA) was used as a protecting or stabilizing agent during the self-assemble of the cationic polymer and the negatively charged inorganic silica species. With the assistant of in-situ crystallization, the

---

* Corresponding author at: 12# Zhangzhou Road, Zibo City, Shandong Province, 255049, PR China. Tel./fax: +86 533 2786290.
E-mail addresses: yinxiaoyan731027@yahoo.cn, yinxiaoyan731027@163.com (X. Yin).

1566-7367/$ – see front matter © 2013 Elsevier B.V. All rights reserved.
http://dx.doi.org/10.1016/j.catcom.2013.10.007

nanosized precursors turned into MCM-22 nanosized zeolite. The performances of the MCM-22-NZ catalysts in the methane dehydroaromatization (MDA) reaction have also been studied. The results have shown that the synthesized MCM-22-NZ displays superior catalytic properties in comparison with the conventional micro-sized MCM-22 zeolites in MDA reaction.

2. Experimental method

2.1. MCM-22-NZ preparation

All reagents were used as received without further purification. Cationic polymer, PDDA (molecular weight lies in the range of 2 × 105–3.5 × 105, 20 wt.%, purchased from Aldrich) was used for the protecting or stabilizing agent in the synthesis. The MCM-22-NZ was synthesized using hexamethyleneimine (HMI, >99%, purchased from Aldrich) as a structure direction agent (SDA). 0.496 g sodium hydroxide (NaOH, >96%), 0.798 g sodium metaaluminate ($NaAlO_2$, Al_2O_3: >45%), and about 3 g PDDA were mixed in 85 mL deionized water and vigorously agitated for more than 60 min. Then, 15.886 g ludox (AS-40, SiO_2: 40 wt.%, Aldrich) was added carefully into the above mixture by dropping under vigorously agitated condition. After agitating for over 12 h, 5.35 g HMI was added to obtain the final mixture. The resultant mixture was introduced into a stainless-steel autoclave, followed by heating at 343 K for 1 day and then 423 K for 7 days under the condition of rotating crystallization. After quenching the autoclave to room temperature, the solid sample was separated from the mixture by centrifugation, washed by deionized water and then dried at 393 K over night. The SDA and the cationic polymers were removed by calcination in air in a muffle at 823 K for 10 h. For comparison, the synthesis experiment was carried out with the same composition except for the presence of cationic polymers so as to obtain conventional MCM-22 zeolites. The procedure of preparation of Mo/HMCM-22-NZ and Mo/HMCM-22 catalysts was similar with that described in the references [1,22].

2.2. Characterization and catalytic evaluation

The synthesized product was characterized by X-ray powder diffraction (XRD) on a Rigaku-Dmax 2400 diffractometer equipped with graphite monochromatized CuKα radiation in the 2θ angle ranging from 5 to 50° and scanning electron micrograph (SEM, KYKY-2800B). Transmission electron microscopy (TEM) was carried out on a Philips Tecnai G2 20 instrument, operating at 200 kV. The crystal size distribution was determined by dynamic light scattering (DLS) with a ZETASIZER1000 instrument (DTS 5101, Malvern Ltd. Company). Nitrogen adsorption analysis was carried out with a Micromeritics ASAP 2020 adsorption analyzer at 77 K. The X-ray fluorescence (XRF) spectrometry analysis was carried on Bruker SRS-3400 instrument. TG profiles were recorded on a NETZSCH STA 449 C instrument. NH_3 temperature-programmed desorption (NH_3-TPD) was performed on a conventional set-up equipped with a thermal conductivity detector. 0.2 g of the sample was first flushed with He (30 ml/min) at 873 K for 30 min, then cooled to 423 K and saturated with NH_3 until equilibrium. It was then flushed with He again until the baseline of the integrator was stable. NH_3-TPD was then promptly started from 423 to 900 K at 15 K/min.

The MDA reaction was carried out in a continuous flow quartz tubular fixed-bed reactor (8 mm i.d.) at atmospheric pressure and 973 K, a space velocity of 1500 mL/(g·h). The effluents were analyzed by an on-line gas chromatograph equipped with ten-way sampling valve (Valco) for auto-sampling every time per 30 min and the detailed procedures were described in the previous studies [23].

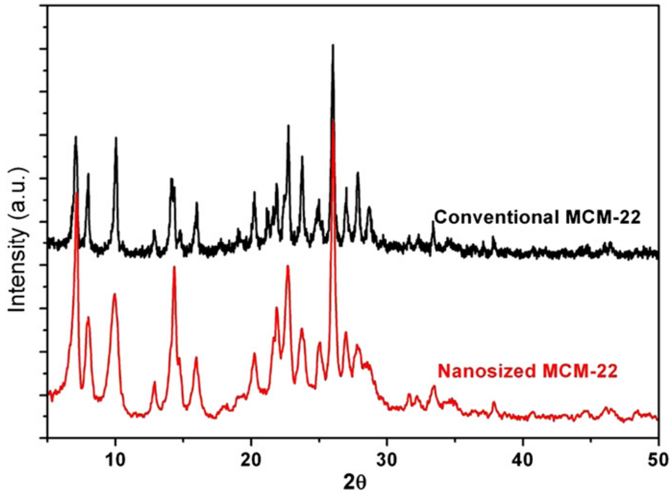

Fig. 1. XRD patterns of the nanosized and conventional microsized MCM-22 zeolites.

3. Results and discussion

3.1. Characterization

Fig. 1 shows the X-ray diffraction (XRD) patterns of the calcined nanosized and conventional micro-sized MCM-22 zeolites. Well-resolved peaks in the 4–40° range are characteristic features of the MCM-22 structure [24,25] without other crystalline phases and

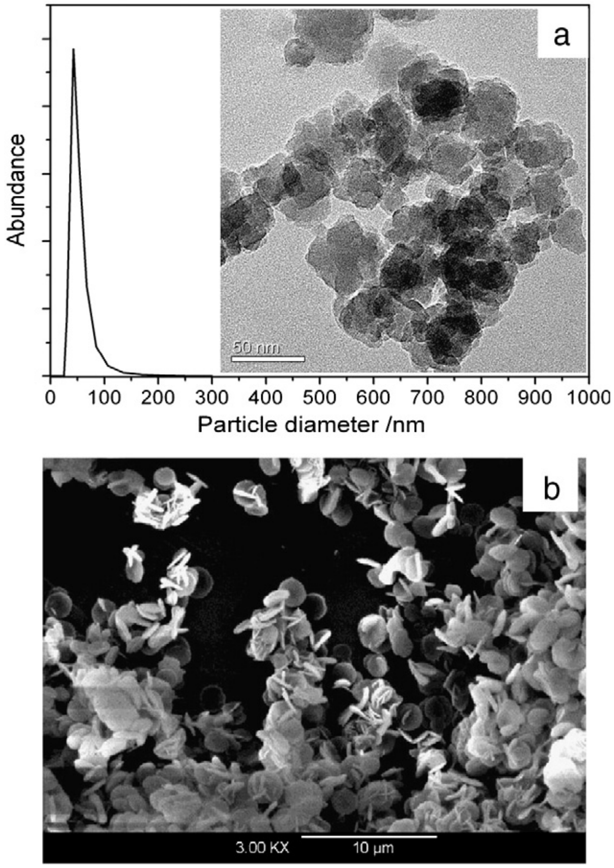

Fig. 2. Particle size distribution determined by DLS (a) and the corresponding TEM image of the MCM-22-NZ (inset figure in a), and SEM image of the conventional microsized MCM-22 zeolites (b).

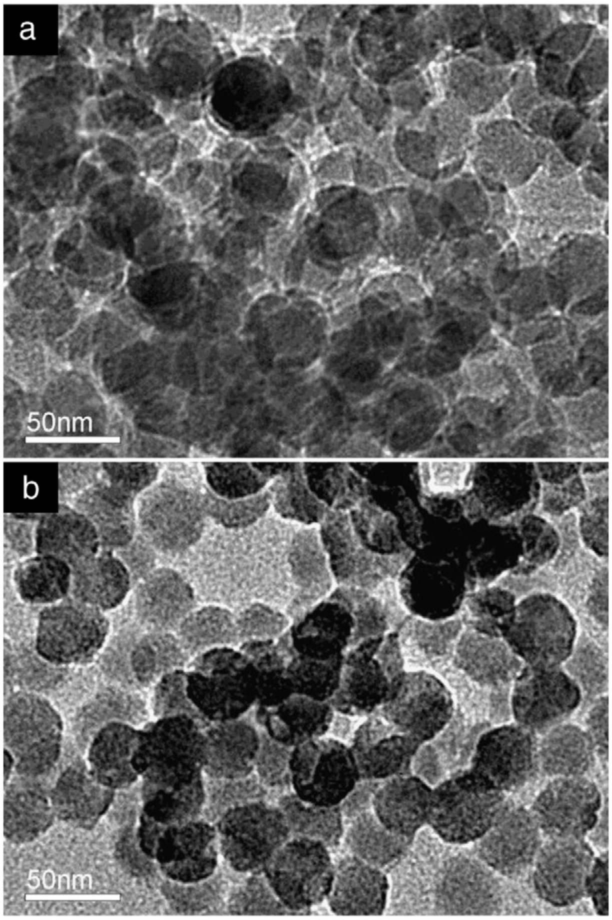

Fig. 3. TEM images of the synthesis colloids without PDDA (a) and with the presence of PDDA (b).

amorphous phase, confirming the formation of MCM-22 zeolites with the high crystallinity. Obviously, the XRD peaks for the nanozeolites are considerably broader than the conventional microsized MCM-22 as the crystal size decrease according to Scherrer equation, indicating the formation of the MCM-22-NZ.

TEM and DLS have been adopted to determine the crystal size distribution, and the results are shown in Fig. 2a. It is estimated that the MCM-22-NZ obtained in this work possesses an average size of 40–50 nm with a narrow particle size distribution as determined by DLS. The TEM image presents very uniform crystal particle with crystal sizes of about 40 nm, which matches the result of DLS.

3.2. Growth mechanism

Different from the nanosized MCM-22 shown in Fig. 2a, the conventional MCM-22 zeolite synthesized in the control experiment shows uniform platelet-like crystals of about 2 μm in size (Fig. 2b). This indicates cationic polymer, PDDA, plays the crucial role in the synthesis process of the MCM-22-NZ. It has been reported that Ludox (SiO_2 particles) can be used as the coating nanoparticles by electrostatically self-assembly with PDDA to achieve the desired topology and structure. Additionally, the cationic polymer is often used to modify substrate surface by exploiting the electrostatic attraction for their deposition [26–28]. Because of the electrostatic stabilization effect, polyelectrolytes can also be used as stabilizing agents for colloids to avoid the self-aggregation [29,30].

In this work, PDDA really plays the vital role of protection agent to avoid the synthesis colloids self-aggregation. Fig. 3 shows the TEM images of the synthesis colloids with and without the presence of PDDA. Clearly, compared with the synthesis colloids without PDDA (Fig. 3a), dispersive nano-silica species can be identified in the image with the presence of PDDA (Fig. 3b). This is attributed to the existence of the cationic polymer PDDA, which can effectively interact with negatively charged inorganic silica species in the synthesis system due to the electrostatically self-assembly. Moreover, during the rotating crystallization process, PDDA prevents the inorganic silica species

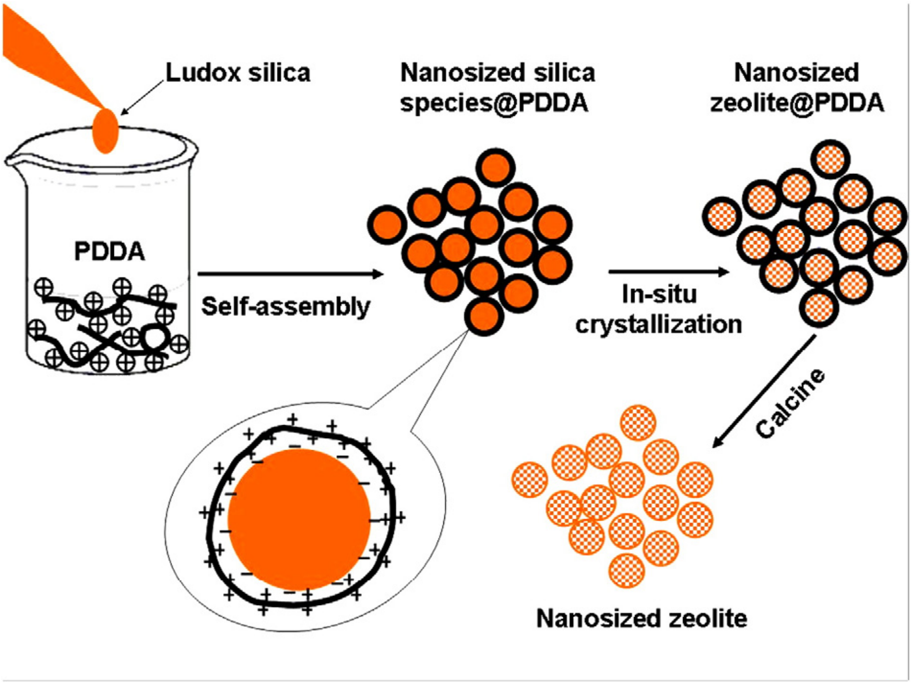

Fig. 4. Schematic diagram for the synthesis of MCM-22-NZ by the facile strategy combined self-assembly with in-situ crystallization.

from self-aggregation and intergrowth. It is well known that the architecture of silica precursor impacts the morphology of the result zeolite crystals considerably after nucleation and crystallization. From the results of our experiment, the amount of PDDA can effectively impact the interaction between PDDA and Ludox. So, the size of the colloids can be controlled by varying the amount of PDDA. The intensive research work is carrying out in our laboratory now and the results were not shown in this paper.

By using our proposed method, the separated nanosized crystals can be obtained successfully after in-situ crystallization. The rationale of this method can be illustrated by the schematic diagram in Fig. 4. The demonstrated procedure of MCM-22-NZ synthesis involves three major steps: i) formation of the isolated small precursor particles using PDDA as protecting or stabilizing agent by self-assembly of the cationic polymer and the negatively charged inorganic silica species; ii) in-situ crystallization of the nanosized precursors into nano-zeolite; iii) removal of the cationic polymers.

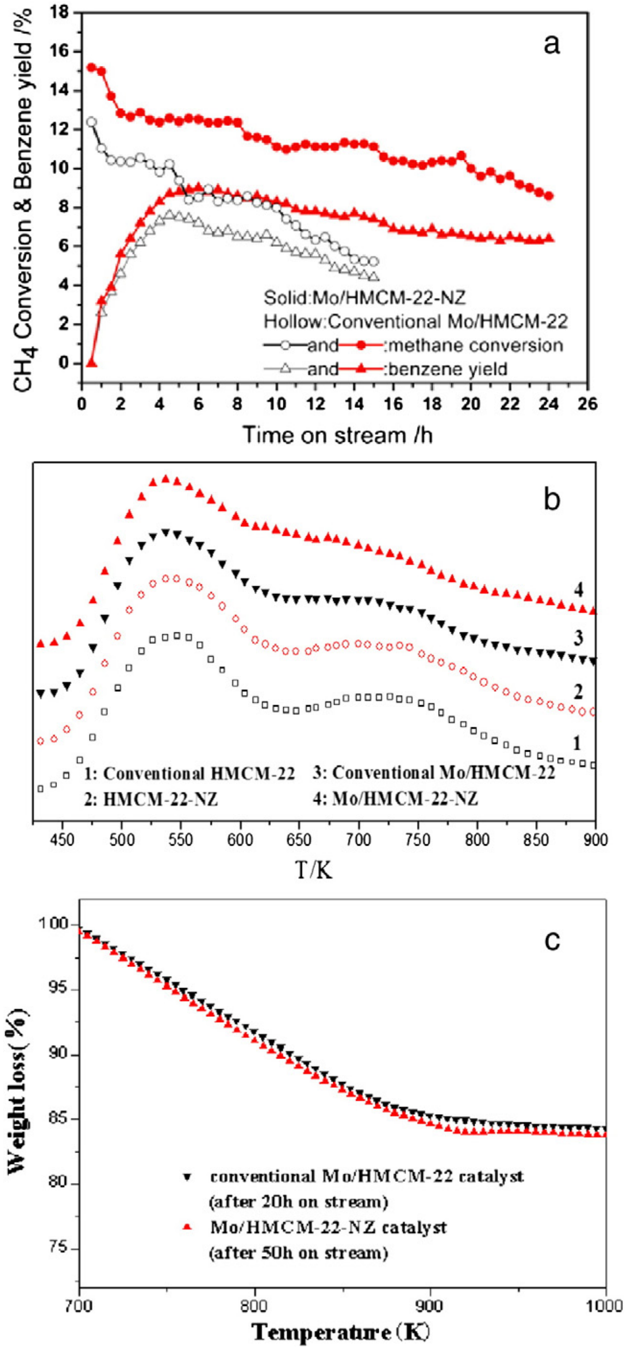

Fig. 5. The catalytic performance comparison for Mo/HMCM-22-NZ catalyst and conventional Mo/HMCM-22 catalyst in MDA reaction (a), NH_3-TPD spectra of the different catalysts (b), and TG profiles of the coked catalysts (c).

3.3. Catalytic evaluation

The catalytic activity of MCM-22-NZ in methane dehydroaromatization (MDA) reaction was also studied in this paper. Fig. 5(a) presents the properties of MCM-22-NZ and conventional micro-sized MCM-22 zeolites synthesized in this study over Mo-based catalyst in MDA reaction. It was reported that the optimized Mo content was 6 wt.% for Mo/HMCM-22 catalysts [1,6]. Therefore, Mo content 6 wt.% was chosen for both nanosized Mo/HMCM-22 and conventional microsized Mo/HMCM-22 catalysts. Under the same employed reaction conditions, significant improvement in the catalytic performance of the MDA reaction has been observed for the nanosized Mo/HMCM-22. The MCM-22-NZ catalyst exhibited much higher CH_4 conversion and much higher yield of benzene (increased about 30%) than those of the conventional Mo/HMCM-22 catalysts synthesized in the present work. The Mo/HMCM-22-NZ catalyst still displays good catalyst stability with the benzene yield of over 6% until the reaction runs for 24 h. On the contrary, for the conventional microsized Mo/HMCM-22 catalyst, a heavier coke deposit leads to a rapid decrease of the methane conversion with time-on-stream.

The XRF analysis of the conventional Mo/HMCM-22 and Mo/HMCM-22-NZ catalysts is listed in Table 1, which results show that the Mo/HMCM-22-NZ possesses the similarity to the conventional Mo/HMCM-22 catalyst in terms of SiO_2/Al_2O_3 ratio and Mo content. The NH_3-TPD results of the conventional HMCM-22, HMCM-22-NZ, the conventional Mo/HMCM-22 and Mo/HMCM-22-NZ (Fig. 5b) in our work show the similarity of both types and areas of peaks. Besides, the results are reasonably consistent with that reported by Bao [1], and the peak at about 518 K (peak L) was attributed to the desorption of the physisorbed NH_3 species and/or NH_3 adspecies residing on non-exchangeable cationic sites, while the peak at 627 K (peak H) was assigned to the desorption of NH_3 adspecies adsorbed on exchangeable protonic sites, i.e., Brönsted acid sites. Compared to HMCM-22 and HMCM-22-NZ, Mo/HMCM-22 and Mo/HMCM-22-NZ showed a decreased high-temperature peak. The shape of high-temperature peaks of Mo/HMCM-22 and Mo/HMCM-22-NZ are similar and the intensity of the latter was slightly weaker than that of the former.

Taking into account that there is no post-treatment or post-synthesis adopted to improve the catalytic performance, and the Mo/HMCM-22-NZ catalyst possesses the similarity to the conventional catalyst in terms of SiO_2/Al_2O_3 ratio, Mo content and the acidity, the high activity and exceptional stability of Mo/HMCM-22-NZ catalyst are reasonably attributed to the nanosized effect of the catalyst particle. The BET surface areas and pore volumes of traditional MCM-22 and MCM-22-NZ are listed in Table 2. For the traditional MCM-22 synthesized in this work, the data are similar with those reported in literatures 1 and 31. While, the BET surface area of MCM-22-NZ (491 m^2/g) is higher than that of the traditional MCM-22 (448 m^2/g). The nanocrystal MCM-22-NZ with morphology of polycrystalline grains also generates the secondary pores from intercrystal gap of nanoscale MCM-22-NZ. So, the nanosized MCM-22-NZ

Table 1
Results of XRF analysis of the conventional Mo/HMCM-22 catalyst and the Mo/HMCM-22-NZ catalyst.

Catalysts	Mo (wt.%)	SiO_2 (wt.%)	Al_2O_3 (wt.%)	$[SiO_2/Al_2O_3]$
Mo/HMCM-22	5.9	85.3	5.1	28.4
Mo/HMCM-22-NZ	6.0	84.7	5.04	28.6

Table 2
BET surface areas and pore volumes of the conventional MCM-22 and MCM-22-NZ.

Sample	Si/Al ratio	Surface area (m^2/g)	Micropore area (m^2/g)	Micropore volume (cm^3/g)	Reference
MCM-22	30	458	352	0.16	[1]
MCM-22	15	453	335	0.15	[31]
MCM-22	15	448	356	0.16	This paper
MCM-22-NZ	15	491	359	0.17	This paper

catalyst can possess higher surface activity and lower tendencies to carbon deposition, which lead to the remarkable increase in the catalytic durability. Furthermore, the nanosized MCM-22, because of its small size, has shorter diffusion path length and easier access for the reactant, increases the diffusion rate of molecules and shortens the residence time of molecules in channels of nanocrystal, resulting in the higher CH_4 conversion.

TG analysis of the coked catalysts also confirmed that the nanosized MCM-22 catalyst can favor strong coking-resistance and result in strong catalyst stability. TG profiles of the coked Mo/HMCM-22 and Mo/HMCM-22-NZ catalysts were shown in Fig. 5c. The coked Mo/HMCM-22 catalyst shows a weight loss of about 15% after 20 h on stream. By contrast, the coked Mo/HMCM-22-NZ catalyst displays about 16% weight loss after 50 h on stream. Therefore, the average rate of coke formation on the Mo/HMCM-22-NZ catalyst (about 0.32% per hour) is lower than the 0.75% coke formation rate of the Mo/HMCM-22 catalyst. These results demonstrate that the Mo/HMCM-22-NZ catalyst possesses much better tolerance to carbonaceous deposits, which is favorable to strong catalyst stability.

Mo/HMCM-22-NZ plays the important role of high quality bifunctional catalysts in MDA reaction. It is well known that there is an induction period in the early stage of the reaction in which the MoO_3 species are reduced by CH_4 into Mo_2C species, accompanied by the depositing of carbonaceous cokes (carbonaceous deposits associated with molybdenum). The transformation of molybdenum oxide to molybdenum carbide is dominant for this period. It is reasonable that much carbonaceous deposits associated with molybdenum occur in the early reaction stage. Moreover, the formed Mo_2C species are active species for CH_4 activation and can continuously activate CH_4 to produce active intermediates. Subsequently, the active intermediates are condensed on the acid site of catalysts and benzene is produced. At the same time, the aromatic coke deposits form on the acid site, which would lead to the deactivation of the catalyst.

Compared to the conventional Mo/HMCM-22 catalyst, the nanostructure of the Mo/HMCM-22-NZ catalyst is beneficial to the well-distribution of the Mo active species on the zeolite support. So, Mo active species can have the efficient combination with the zeolite acidic sites. Furthermore, Mo/HMCM-22-NZ provides easier access to the active sites for both reactant and larger product molecules like benzene. The fast transport of larger products is in favor for improving both catalyst activity and durability of catalyst as reported by literature works [32–35]. Therefore, high quality bifunctional catalyst (Mo/HMCM-22-NZ) naturally gives rise to higher methane conversion, higher benzene yield and stronger catalyst stability in comparison with the conventional Mo/HMCM-22 catalyst.

4. Conclusions

The new route of combination self-assembly with in-situ crystallization techniques was proposed to facilely prepare nano-sized MCM-22 zeolite catalysts (MCM-22-NZ). In this route, PDDA prevents the inorganic silica species from self-aggregation and intergrowth, and finally very uniform MCM-22 crystal particles with crystal sizes of about 40 nm could be obtained easily after rotating crystallization. From the results of N_2 adsorption and TG analysis, the nano-sized MCM-22-NZ catalysts possess higher surface activity and lower tendencies to carbon deposition compared to the conventional micro-sized MCM-22 catalysts. Therefore, the MCM-22-NZ catalyst displayed higher methane conversion, higher benzene yield and stronger catalyst stability in methane dehydro-aromatization (MDA) reaction compared to the conventional micron scale catalyst. This work revealed a new and feasible way for the synthesis of nanosized zeolite catalysts. The demonstrated route may be extended to synthesize other types of zeolite catalysts with unusual structure and properties.

Acknowledgment

The financial supports of the National Key Technology R&D Program (2006BAE02B05) and National Natural Science Foundation of China (21076119 and 21276148) are greatly acknowledged.

References

[1] Y. Shu, D. Ma, L. Xu, Y. Xu, X. Bao, Catal. Lett. 70 (2000) 67.
[2] Y. Xu, X. Bao, L. Lin, J. Catal. 216 (2003) 386.
[3] Z. Sobalík, Z. Tvaruzková, B. Wichterlová, V. Fíla, Š. Špatenka, Appl. Catal. A Gen. 253 (2003) 271.
[4] H. Liu, W. Shen, X. Bao, Y. Xu, Appl. Catal. A Gen. 295 (2005) 79.
[5] A. Hassan, A. Sayari, Appl. Catal. A Gen. 297 (2006) 159.
[6] L. Liu, D. Ma, H. Chen, H. Zheng, M. Cheng, Y. Xu, X. Bao, Catal. Lett. 108 (2006) 25.
[7] C. Delitala, M.D. Alba, A.I. Becerro, Microporous Mesoporous Mater. 118 (2009) 1.
[8] S. Laforge, D. Martin, M. Guisnet, Microporous Mesoporous Mater. 67 (2004) 235.
[9] G. Xu, X. Zhu, X. Niu, Microporous Mesoporous Mater. 118 (2009) 44.
[10] I. Kolev, V. Mavrodinova, M.R. Mihályi, M. Kollár, Microporous Mesoporous Mater. 118 (2009) 258.
[11] X. Dong, Y. Song, W. Lin, Catal. Commun. 8 (2007) 539.
[12] Y. Li, L. Liu, X. Huang, X. Liu, W. Shen, Y. Xu, X. Bao, Catal. Commun. 8 (2007) 1567.
[13] A.C.C. Rodrigues, J.L.F. Monteiro, Catal. Commun. 9 (2008) 1060.
[14] L. Tosheva, V.P. Valtchev, Chem. Mater. 17 (2005) 2495.
[15] S.C. Larsen, J. Phys. Chem. C 111 (2007) 18464.
[16] M. Firoozi, M. Baghalha, M. Asadi, Catal. Commun. 10 (2009) 1582.
[17] L. Sun, X. Guo, G. Xiong, X. Wang, Catal. Commun. 25 (2012) 18.
[18] W. Song, R.E. Justice, C.A. Jones, V.H. Grassian, S.C. Larsen, Langmuir 20 (2004) 8301.
[19] W. Song, V.H. Grassian, S.C. Larsen, Chem. Commun. (2005) 2951.
[20] I. Schmidt, C. Madsen, C.J.H. Jacobsen, Inorg. Chem. 39 (2000) 2279.
[21] S. Kim, J. Shah, T.J. Pinnavaia, Chem. Mater. 15 (2003) 1664.
[22] H. Liu, L. Su, H. Wang, W. Shen, X. Bao, Y. Xu, Appl. Catal. A Gen. 236 (2002) 263.
[23] N. Chu, J. Yang, J. Wang, S. Yu, J. Lu, Y. Zhang, D. Yin, Catal. Commun. 11 (2010) 513.
[24] Y. Wu, X. Ren, Y. Lu, J. Wang, Microporous Mesoporous Mater. 112 (2008) 138.
[25] Y. Wu, X. Ren, J. Wang, Microporous Mesoporous Mater. 116 (2008) 386.
[26] F. Caruso, R.A. Caruso, H. Möhwald, Science 282 (1998) 1111.
[27] F. Caruso, H. Lichtenfeld, M. Giersig, H. Möhwald, J. Am. Chem. Soc. 120 (1998) 8523.
[28] G. Decher, Science 277 (1997) 1232.
[29] S. Chen, Langmuir 15 (1999) 7551.
[30] H. Chen, Y. Wang, Y. Wang, S. Dong, E. Wang, Polymer 47 (2006) 763.
[31] A. Corma, V. Martinez-Soria, E. Schnoeveld, J. Catal. 192 (2000) 163.
[32] W. Li, A. Lu, R. Palkovits, W. Schmidt, B. Spliethoff, F. Schüth, J. Am. Chem. Soc. 127 (2005) 12595–12600.
[33] F. Schüth, Annu. Rev. Mater. Res. 35 (2005) 209–238.
[34] F.S. Xiao, L. Wang, C. Yin, K. Lin, Y. Di, J. Li, R. Xu, D.S. Su, R. Schlgl, T. Yokoi, T. Tatsumi, Angew. Chem. Int. Ed. 45 (2006) 3090–3093.
[35] K. Egeblad, C.H. Christensen, M. Kustova, C.H. Christensen, Chem. Mater. 20 (2008) 946–960.